Improvement of Frequency Fluctuations in Microgrids Using an Optimized Fuzzy P-PID Controller by Modified Multi Objective Gravitational Search Algorithm

H. Shayeghi*(C.A.) and A. Ghasemi*

Abstract: Microgrids is an new opportunity to reduce the total costs of power generation and supply the energy demands through small-scale power plants such as wind sources, photo voltaic panels, battery banks, fuel cells, etc. Like any power system in micro grid (MG), an unexpected faults or load shifting leads to frequency oscillations. Hence, this paper employs an adaptive fuzzy P-PID controller for frequency control of microgrid and a modified multi objective Chaotic Gravitational Search Algorithm (CGSA) in order to find out the optimal setting parameters of the proposed controller. To provide a robust controller design, two non-commensurable objective functions are formulated based on eigenvalues-domain and time-domain and multi objective CGSA algorithm is used to solve them. Moreover, a fuzzy decision method is applied to extract the best and optimal Pareto fronts. The proposed controller is carried out on a MG system under different loading conditions with wind turbine generators, photovoltaic system, flywheel energy, battery storages, diesel generator and electrolyzer. The simulation results revealed that the proposed controller is more stable in comparison with the classical and other types of fuzzy controller.

Keywords: Microgrid, Frequency control, Multi objective CGSA, Adaptive fuzzy P-PID controller.

1. Introduction

1. 1. Objective of the Study

With regard to global warning of greenhouse gases, the microgrids (MGs) can be considered for future electric power systems consisting of small-scale power units, energy storage systems and loads [1]. In other words, MGs provide the appropriate grounds for high-penetration of renewable energies and distributed energy resources (DER) [2]. Noted that the MG is essentially a nonlinear small-scale power system and undergo a wide range of transient conditions will face some stability problems. Therefore, sufficient damping of frequency oscillations is important in MG [3].

1. 2. Literature Review

In the last two decades many studies have been conducted on the MGs [3-6]. In some of them the classical controllers were employed to enhance the frequency oscillations in MGs [4-5]. It is clear that a fixed controller based on the classical theories is not suitable for frequency control of microgrid. Considering the MG frequency control problem, the conventional control strategies take the integral of the area control error as the control signal. An integral controller can achieve a zero steady state deviation; however, it exhibits poor dynamic performance [6]. To cope with this aim, many researchers presented the PID-type fuzzy controller designing and its derivations [7-8]. Compared to the conventional strategies, fuzzy logic controller (FLC) provides much better results; however, it requires fine-tuning and hard efforts to achieve effective performance to damp out the frequency fluctuations. In Ref. [9], a robust fuzzy-PID control system established by incorporating an optimal fuzzy reasoning into a well-developed PID-type FLC. Although, this type of controller is more effective than the classical controllers, the well optimized fuzzy controller can be resulted in more stability. Therefore, optimization algorithm is certainly the first option in this case to reduce fuzzy system effort and find better fuzzy controller [10-12].

In order to control isolated MG, some researchers have used droop control strategies based on active power and frequency (p-f) curve derived from distributed generation (DG) converters. In Ref. [13], a droop control strategy was suggested for DG resources to control the MG frequency. Moahmadi et al. [14] presented a novel method

Iranian Journal of Electrical & Electronic Engineering, 2016.
Paper received 8 August 2016 and accepted 23 October 2016.
* The Authors are with the Technical Engineering Department, University of Mohaghegh Ardabili, Ardabil, Iran.
E-mail: hshayeghi@uma.ac.ir, ghasemi.agm@gmail.com
Corresponding Author: H. Shayeghi.

based on droop control strategy of photovoltaic and battery converters to control the MG frequency. This strategy was evaluated by some virtual MGs and the results revealed an acceptable performance with respect to the MG frequency control problems. In Ref. [15], the torque and frequency droop control strategies are used for a doubly-fed induction generator (DFIG). Yuen et al. [16] also stated the practical aspects of providing frequency control reserves (FCRs) and the potential economic profitability of participating in FCR markets based on a setup of multiple MGs. In addition, Ref. [17] was dedicated to a new energy management system (EMS) model to improve the security of a MG in a cost-effective manner. In Refs. s[18, 19], the role of a cascaded H-bridge (CHB) multilevel converter in controlling the frequency was examined. In Ref. [20], investigations were carried out on the coordinated vehicle-to-grid (V2G) control and frequency controller for robust frequency control in a smart grid with large penetration of renewable energy sources (RES). Here, the battery state-of-charge (SOC) was controlled by the optimized SOC deviation. Li et al. [21] focused on the feasibility of electrolyzer and fuel-cell hybrid system control to secure a real power balance and increase the operational capability of the load frequency control model. In Ref. [22], a virtual synchronous generator control method was reported to use the same control method in standalone and grid-connected operations. Authors in Ref. [23] proposed a battery energy storage system to maintain the frequency control process within MGs with large penetration of RES. In this study, it was concluded that the final solution improves the system's stability and security of supply. Shafiee et al. [24] suggested a new method to consider the secondary controls in the droop-controlled MGs.

1. 3. Motivation and contribution

In this paper an adaptive fuzzy P-PID controller is proposed for frequency control of MG. As the optimizing of the proposed fuzzy controller is very important to achieve the desired level of system performance, a modified gravitational search algorithm (GSA) is used to optimize fuzzy P-PID structure. Because, the GSA is a well-known and successful algorithm with flexible structure [25-27]. In order to resolve its shortcomings to obtain the global optimum solution and ensure the solutions not being trapped in local optima when system has a highly epistatic objective function and number of to be optimized variables is large, a new modified multi objective GSA-based CLS operator, called the CGSA, is investigated to optimize the parameters of the proposed fuzzy controller. The proposed fuzzy P-PID model is a flexible controller with simple configuration that is easy to implementation. As results, the main contributions of this paper can be summarized as follows:

i) Suggestion a fuzzy P-PID controller to improve frequency fluctuation of a MG
ii) Presenting a modified gravitational search algorithm based on the chaos theory to optimize the proposed fuzzy controller parameters.
iii) Considering the nonlinear components and inherent uncertainties of the MGs in synthesis procedure.
iv) Analyzing the MG system equipped with the proposed fuzzy controller under sever operating conditions and power generation uncertainties.

1. 4. Outline of this paper

The rest outline of this paper is structured as follows. Section 2 illustrates the proposed MG and fuzzy P-PID controller structure. Section 3 introduces the multi objective CGSA algorithm and section 4 shows the consistency of two previous sections with respect to the frequency stability. Section 5 describes several loading conditions to demonstrate the performance of the proposed fuzzy P-PID controller in a MG. Finally, the paper is concluded in Section 6.

2. The proposed power system model

2. 1. Microgrid configuration

The real configuration of the studied MG is shown in Fig. 1 and the block diagram of this system is shown in Fig. 2 [1]. As shown in Fig. 1, MG is an interconnection of domestic distributed loads and low voltage distributed energy sources, such as microturbines, wind turbines, PVs, storage devices, diesel generator, and electrolyzer system. It consists of a group of radial feeders as a part of a distribution system. The domestic load can be divided to sensitive/critical and nonsensitive/noncritical loads via separate feeders. The sensitive loads must be always supplied by one or more microsources, while the nonsensitive loads may be shut down in case of contingency, or a serious disturbance. Each unit's feeder has a circuit breaker and a power flow controller commanded by the central controller or energy manager. The circuit breaker is used to disconnect the correspondent feeder (and associated unit) to avoid the impacts of sever disturbances through the MG. The ac MG can be connected to the distribution system by a point of common coupling (PCC) via a static switch (SS). The static switch is capable to island the MG for maintenance purposes or when faults or a contingency is occurred.

For the feeders with sensitive loads, local power supply, such as diesel generators or energy capacitor systems (ECSs) with enough energy saving capacity are needed to avoid interruption of electrical supply. An MG central controller (MGCC) facilitates a high level management of the MG operation by means of technical and economical functions. The microsource controllers (MCs) control the microsources and the energy storage systems. Finally, the controllable loads are controlled by load controllers (LC). The microsources and storage devices use power

electronic circuits to connect to the ac MG. Usually, these interfaces depending to the type of unit are ac/ac, dc/ac, and ac/dc/ac power electronic converters/inverters. As the MG elements are mainly power-electronically interfaced, the MG control depends on the inverter control. For increasing reliability in the conventional power systems, the MG systems must be able to have proper performance in both connected and disconnected modes. In connected mode, the main grid is responsible for controlling and maintaining power system in desired conditions and, the MG systems act as real/reactive power injectors. But in disconnected mode, the MG is responsible for maintaining the local loads and keeping the frequency and voltage indices at specified nominal values. All needed data for the MG is given Appendix A [28].

In the simulation, the nonlinear model (Fig. 3) with ±0.1 saturation values is replaced with the linear model of turbine ΔPVki/ΔPTki represented in Fig, 2 to take the generation rate constraint (GRC), i.e. the practical limit on the rate of change in the generating power, into account.

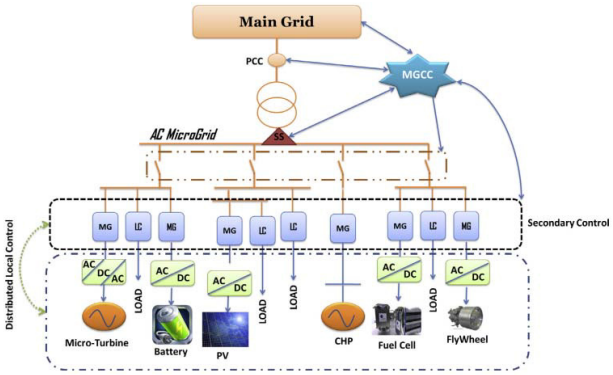

Fig. 1. The Proposed microgrid containing different types of power plants

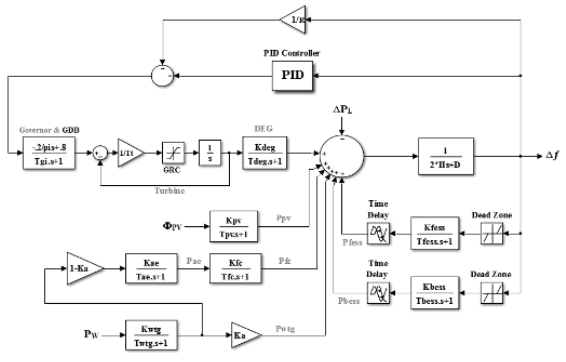

Fig. 2. Block diagram of the microgrid system

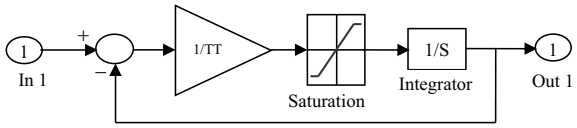

Fig. 3. Nonlinear turbine model with GRC

Figure 4 shows the structure of the governor concerning the Governor Dead-Band (GDB).

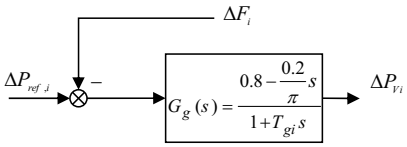

Fig. 4. A nonlinear model of governor with GDB

Note that these types of power plants have inherent uncertainties or nonlinear pattern; however, to the best knowledge of the researcher, few studies have examined this issue. This paper presents a modified GSA algorithm to design a P-PID fuzzy controller for load frequency control considering GDB, GRC and RES system uncertainties. This model can be considered as real-time potential of the studied MG.

2. 2. Adaptive Fuzzy P-PID controller

The graphical view of the proposed adaptive fuzzy P-PID damping controller with a global signal Δf is shown in Fig. 5. The membership functions are used to specify a set of rules, called the rule base which developed based on the optimization procedure. Rules are developed based on two inputs and three linguistic terms. In an inference model, all the rules are compared to the inputs to decide which rules are relevant in the current condition. After the corresponding process, the necessary rules are extracted and the controlled output is specified for the different input conditions. The de-fuzzification mechanism produces the final crisp output of FLC with regard to the fuzzified input. In Fig. 5, the tracking Δf is the input of the fuzzy inference system. The membership functions for Δf and , and the output kfuzzy are of the conventional triangular kind. In practice, most of the physical systems have inherent tractable characteristics such as high-order and nonlinearity. Therefore, the PID controllers are added to meet the performance demand and multi objective CGSA method is used to optimize the fuzzy P-PID parameter. In other words, the proposed controller consists of the fuzzy P and the conventional PID with low-pass filter. The component fuzzy P tend to make a system faster. The derivative part of PID is used to reduce the rapid

changes and overshoots of the control inputs caused by practical constraints. To deal with the steady-state error and to reject disturbances in the control system, the integral part has been used. The parallel fuzzy P +PID control action can be obtained by algebraically simultaneous summing up the fuzzy P control and PID control actions. In the fuzzy P-PID model, the control effort can be determined by:

$$u = k_{fuzzy} + K_p \Delta f + K_I \int \Delta f + K_D \times \frac{d\Delta f}{dt} = k_{fuzzy} + u_{PID} \tag{1}$$

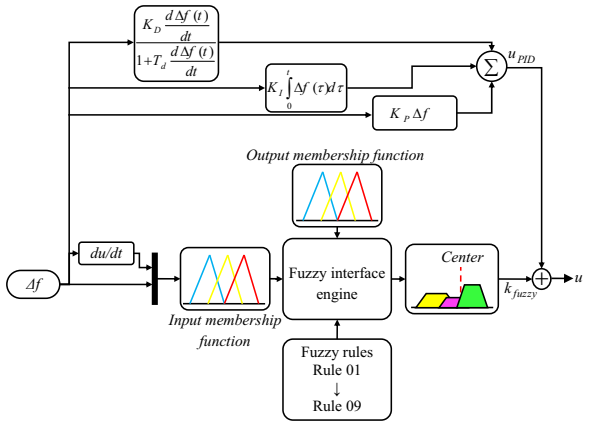

Fig. 5. Block diagram of the proposed fuzzy P-PID controller of the interconnected microgrid

On the other hand, real-world power industry is too conservative to open the well-known PID control loop and replace by a new control technology. In response to this challenge, in the present paper, the PID controller is remained, and the MGSA-based fuzzy logic is used for online optimal tuning of its parameters. Therefore, this control configuration provides a smooth performance in start-up and transient circumstances and it could be more acceptable for the real-time MG application.

3. Multi objective chaotic gravitational search algorithm

3.1. Standard GSA

In this section, the standard (single-objective) GSA is briefly discussed. In order to get more details, refer to Ref. [25]. To describe the original GSA, consider a vector with s agents (is ith mass in the dth dimension) and the position of ith mass is calculated by:

$$X_i = (x_i^1, ..., x_i^d, ..., x_i^n), i = 1, 2, ..., s \tag{2}$$

Then, mass of ith agent is calculated as follows:

$$M_i(t) = \frac{q_i(t)}{\sum_{j=1}^{s} q_i(t)} \tag{3}$$

where, Mi(t) and qi(t) are the mass value of the ith agent at time t and the gravitational masse, respectively. The qi (t) can be calculated by:

$$q_i(t) = \frac{fit_i(t) - worst(t)}{best(t) - worst(t)} \tag{4}$$

where, fiti(t), worst(t) and best(t) are the fitness value of the ith agent at time t, worst and best fitness, one gets:

$$\begin{cases} worst(t) = \underset{j \in \{1,...,s\}}{Max}\ fit_i(t) \\ best(t) = \underset{j \in \{1,...,s\}}{Min}\ fit_i(t) \end{cases} \tag{5}$$

To calculate the acceleration of the agent i, aid(t), total forces Fid(t) from a set of heavier masses should be obtained based on the gravity law as follows:

$$\begin{cases} F_i^d(t) = \sum_{j \in kbest, j \neq i} rand_i G(t) \frac{M_j(t) M_i(t)}{R_{ij}(t) + \varepsilon} (x_j^d(t) - x_i^d(t)) \\ a_i^d(t) = \frac{F_i^d(t)}{M_i(t)} = \sum_{j \in kbest, j \neq i} rand_j G(t) \frac{M_j(t)}{R_{ij}(t) + \varepsilon} (x_j^d(t) - x_i^d(t)) \end{cases} \tag{6}$$

Then, the next velocity of the agent and its position is computed as:

$$V_i^d(t+1) = rand_i \times v_i^d(t) + a_i^d(t) \tag{7}$$

$$x_i^d(t+1) = x_i^d(t) + v_i^d(t+1) \tag{8}$$

where, randi and randj are two uniformly distributed random numbers in the interval [0, 1], Rij(t) is the Euclidean distance between two agents i and j, Rij(t)=||Xi(t), Xj(t)||2, ε is a small value, kbest is the set of first K agents with the best fitness value and biggest mass as a function of time with the initial value K0 at the beginning which is decreased with time. Here, K0 is set to the total number of agent's s and is linearly reduced to 1. G denotes the

gravitational constant by G0, and can be updated by:

$$G(t) = G(G_0, t) \tag{9}$$

The pseudo code of the standard GSA is shown in Fig. 6.

1. Search space identification, t=0;
2. Randomized initialization Xi(t)
   For i=1,2,…,N;
3. Fitness evaluation of agents;
4. Update G(t), best (t), worst(t) and Mi(t)
   For i=1,2,…,N;
5. calculation of acceleration and velocity;
6. Updating agent's position to yield Xi(t+1)
   For i=1,2,…,N; t=t+1;
7. Repeat steps 3 to 7 until the stopping criterion is reached.

Fig. 6. Pseudo code of the standard GSA

3.2. Chaotic GSA

To enhance the algorithm search ability, the chaos theory is employed. If hasty convergence happens, definitely, there is need to an alternative operator to recover the algorithm search. Hereby, the proposed CGSA combines the standard GSA with CLS. Assume that our array of sensors controls the current Cji+1 that is formulated based on forcing the pendulum, by rewriting it from cos(t) to a new form as follows:

$$c_{i+1}^{j} = \begin{cases} 2c_i^j \times (1 + g_{best}^{k-1} / g_{best}^{k}) \times c\cos(2\pi\, g_{best}^{k-1} / g_{best}^{k}), 0.5 < c_i^j \le 1 \\ 0.1c_i^j \times (1 - \cos((1 + g_{best}^{k-1} / g_{best}^{k}))), 0 < c_i^j \le 0.5 \end{cases} \tag{10}$$

where, gkbest refer to the best optimal value in iteration k and controls the local search ability. Thus, the proposed CLS can be stepped as follows:

Step 1: Generate an initial random chaos population as:

$$\begin{aligned} X_{cls}^{0} &= [X_{cls,0}^{1}, X_{cls,0}^{2}, ..., X_{cls,0}^{Ng}]_{1 \times N_g} \\ cx_0 &= [cx_0^1, cx_0^2, ..., cx_0^{Ng}] \\ cx_0^j &= \frac{X_{cls,0}^{j} - P_{j,\min}}{P_{j,\max} - P_{j,\min}}, j = 1,2,...,Ng \end{aligned} \tag{11}$$

where the chaos variable can be generate as follows:

$$\begin{aligned} X_{cls}^{i} &= [X_{cls,j}^{1}, X_{cls,j}^{2}, ..., X_{cls,j}^{Ng}]_{1 \times N_g}, i = 1,2,...,N_{chaos} \\ x_{cls,i}^{j} &= cx_{i-1}^{j} \times (P_{j,\max} - P_{j,\min}) + P_{j,\min}, j = 1,2,...,N_g \end{aligned} \tag{12}$$

Step 2: Determine the chaotic variables

$$\begin{aligned} cx_i &= [cx_i^1, cx_i^2, ..., cx_i^{Ng}], i = 0,1,2,...,N_{choas} \\ cx_{i+1}^{j} &= base\ CLS \quad j = 1,2,...,Ng \\ cx_0^j &= rand(0) \end{aligned} \tag{13}$$

where Nchaos is the number of individuals for CLS. CxiNg is the ith chaotic variable and the Rand() generate a random value in (0,1).

Step 3: Map the decision variables

Step 4: Convert the chaotic variables into decision variables

Step 5: Assess new solution based on the decision variables

3. 3. Non-dominated Sort (NDS)

The NDS method is employed to build the Pareto ranks dividing the solutions into different fronts with different ranks. Then, the classified individual group is ignored and another layer of non-dominated individuals is considered [29]. In primary sorting, each agent is selected and checked to see whether or not it meets the rules given below with respect to any other agent in the population:

$$Obj.1[i] < Obj.1[j] \quad and \quad Obj.2[i] < Obj.2[j], i \ne j \tag{14}$$

where, i and j are the agent numbers. After ranking the whole population, a large fitness value is then assigned to the individuals in the first non-dominated front with rank 1. To maintain the goal of diversity, the sharing strategy is applied and the shared fitness of each individual in the front 1 is obtained. Subsequently, a fitness value being smaller than the minimum shared fitness value of the previous front is assigned to the individuals in the next front. Once again, the sharing strategy is used and the individual shared fitness values in the second front are obtained. The procedure continues until the individual shared fitness values are achieved for all fronts. The sharing function values (Share (dij)) for all first front agents can be calculated as:

$$\mathrm{Share}(d_{ij}) = \begin{cases} 1 - (\frac{d_{ij}}{\mu_{share}})^2, if \quad d_{ij} < \mu_{share} \\ 0 \qquad\qquad ,otherwise \end{cases} \tag{15}$$

$$d_{ij} = \sqrt{\sum_{a=1}^{P_n} (\frac{x_s^i - x_s^j}{x_s^{\max} - x_s^{\min}})^2} \tag{16}$$

where, p1 is the total number of decision variables, xs is the value of sth decision variable; i and j are the agent numbers. The μshare stands for the maximum distance allowed between any two agents to become members of a niche. In additions, the niche count for the total population (N) is calculated as follows:

$$Nichecount_i = \sum_{j=1}^{N} \text{Share}(d_{ij}) \tag{17}$$

3. 4. Best compromised solution

After the Pareto-optimal solutions are calculated then a suitable decision maker is needed to choose one best compromised solution with respect to a specific preference for different applications. Hence, the fuzzy set mechanism as shown in Fig. 7 is use to resolve this problem. Here, a linear membership function ui is defined for each of the objective functions Fi:

$$u_i = \begin{cases} (F_i^{\max} - F_i) \big/ (F_i^{\max} - F_i^{\min}) & F_i^{\max} > F_i > F_i^{\min} \\ 1 & F_i^{\min} \geq F \\ 0 & F_i^{\max} \leq F \end{cases} \tag{18}$$

where, Fimin and Fimax are the minimum and the maximum values of the objective functions, respectively. It is clear that this membership function indicates the achievement degree of the objective functions. The membership function can be normalized for each non-dominated solution k:

$$u^k = \frac{\sum_{i=1}^{o} u^k i}{\sum_{k=1}^{s} \sum_{i=1}^{o} u^k i} \tag{19}$$

where, O and S are the number of objective functions and non-dominated solutions, respectively. The solution with the maximum value of uk will be selected as the best compromised solution. The proposed CGSA convergence analysis is given in Appendix B.

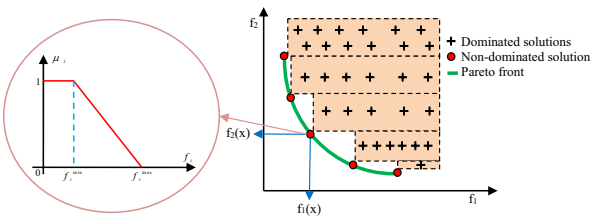

Fig. 7. The FCM method used for the selected Pareto set

4. Optimal tuning of the proposed control strategy

The proposed controller design problem is formulated as a multi objective problem with two conflict objective functions based on time-domain and frequency-domain. The frequency-domain objective function allowed some eigenvalues to be shifted to the left-hand side of the vertical line in the complex plane. The time-domain objective function dictates power system to control the overshot and undershot responded to output frequency in least values. These objective functions are given by:

$$J_1 = \sum_{j=1}^{N_p} \int_0^{t_{sim}} t(\Delta f)dt + \beta \sup(\Delta f) \tag{20}$$

$$J_2 = \sum_{j=1}^{N_p} \max[\text{Re}(\lambda_{i,j}) - \min_{i,j}\{-\zeta \mid \text{Im}(\lambda_{i,j})|, \alpha\}] \tag{21}$$

where, NP, tsim, λ and ζ are the number of operating conditions, the time of simulation¸ the ith eigenvalue of the system at an operating point and the desired minimum damping, respectively. Here, α and β are sets with constant values 0.56 and 0.085, respectively. The optimal tuning parameters problem can be expressed by:

$$\begin{aligned} &Minimize\ [J_1, J_2]\ \ Subject\ to: \\ &K_p^{\min} \leq K_p \leq K_p^{\max} \quad K_I^{\min} \leq K_I \leq K_I^{\max} \\ &K_D^{\min} \leq K_D \leq K_D^{\max} \quad w^{\min} \leq w \leq w^{\max} \end{aligned} \tag{22}$$

The range [0-20] is typically assumed for KP, KI and KD. Moreover, in the proposed model, each agent is formed to indicate the membership functions (MFs) of the fuzzy logic controller's inputs and outputs. In other words, the fuzzy P-PID controller is a fuzzy inference model that maps the given inputs in fuzzy variables subjected to fuzzy membership function. Assuming a priori as the most appropriate fuzzy set covering the domains of quantitative attributes the fuzzy association of MFs mining is difficult. It is usually impractical for experts to represent such sets and finding the most appropriate fuzzy MFs sets. Existing clustering-based automated methods are not of interest because they do not consider the optimization of the discovered membership functions; therefore, the tuning of multi-scheme MFs with n inputs has received a considerable attention and is presented by m1, m2,.., mn. In this regard, some assumptions are considered and scheduled as follow:

i) All MFs are defined as triangular partitions with seven segments from -1 to 1. Zero is the central membership function centered at zero.
ii) Scaling factors of input/output are optimized by using the CGSA.

The above assumptions are presented in Fig 8.

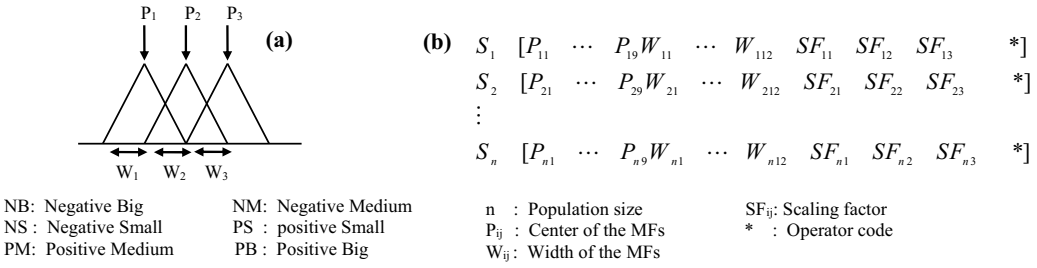

Fig. 8. (a) Symmetrical membership functions, (b) String architecture in tune of membership functions and scaling factors

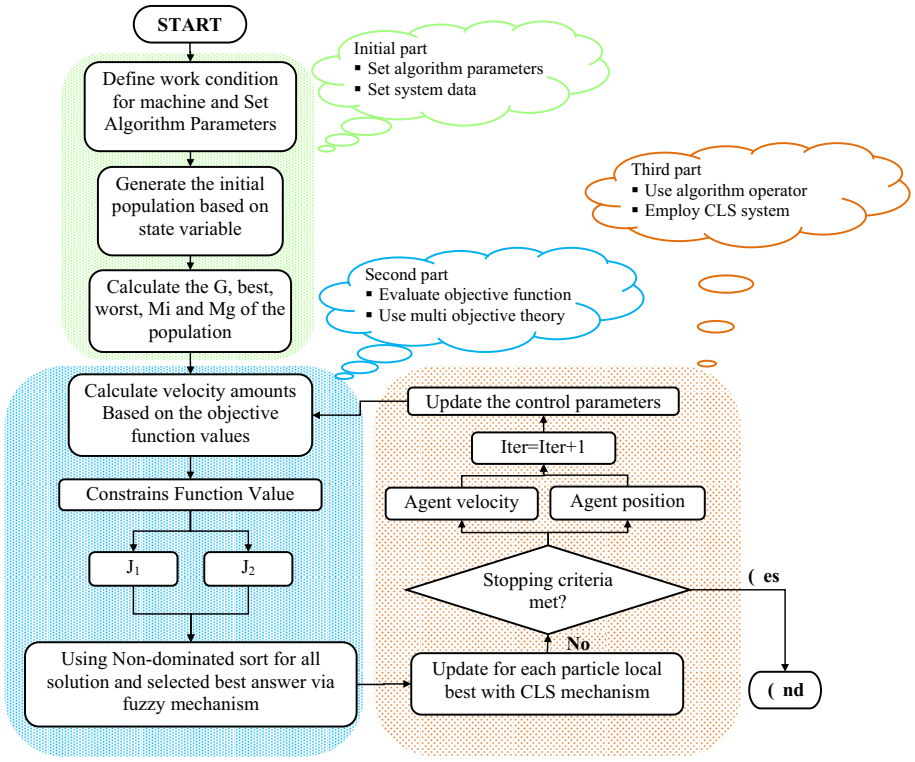

Fig. 9. Flowchart of the proposed algorithm

The combination between optimization of the proposed controller is as follow:

i) The variables are the standard deviation and mean values of each fuzzy MFs.
ii) These variables act as solutions and search for the global best fitness.
iii) It initiates with an initial set of variables.
iv) After the variables' being tuned by the CGSA, these variables will be used to check the performance of the FLC.
v) This process is repeated until the concerned objective is achieved.

Figure 9 shows the optimization flowchart of the multi objective CGSA method.

5. Simulation Results

The performance of the proposed fuzzy P-PID controller based on the modified gravitational search algorithm is validated for a MG system with different types of resources and storages as shown in Fig. 1. Different operating conditions are considered for this test system which listed in Table 1. In order to acquire a better performance, the agent dimension, population size, G0, and α value are set with 40, 60, 20 and 100, respectively. It should be noted that the CGSA algorithm is run for several times

then the optimal set of the proposed controller is selected. The optimal values for the fuzzy P-PID controller are given in Table 2. Also, Fig. 10 shows the MFs form of the fuzzy P-PID controller tuned by CGSA. Figure 11 shows the distribution of the Pareto front belonging to the optimization process.

Table 1. Operating Conditions

1	Increasing load steps from -10% to +10%
2	Increasing parameter R from -40% to +40%
3	Increasing parameter T_{DEG} from -40% to +40%
4	Decreasing parameter T_{WTG} from +40% to -40%
5	Decreasing parameter T_{PV} from +40% to -40%
6	Considering delay

Table 2. Optimal parameters for fuzzy P-PID controller and CGSA algorithm

K_P	1.03
K_I	2.087
$[Low_{limit}\ Up_{limit}]$	[0 , 5]
K_D	6.023

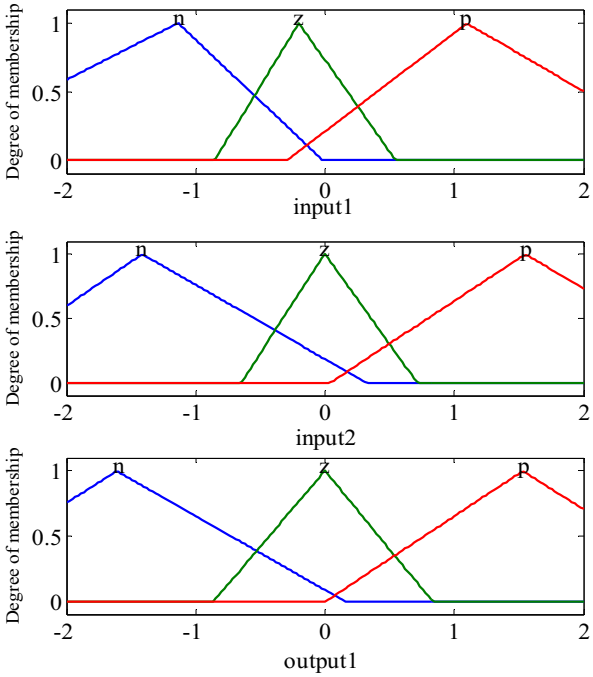

Fig. 10. Optimized MFs for fuzzy logic integrated with the proposed fuzzy P-PID controller

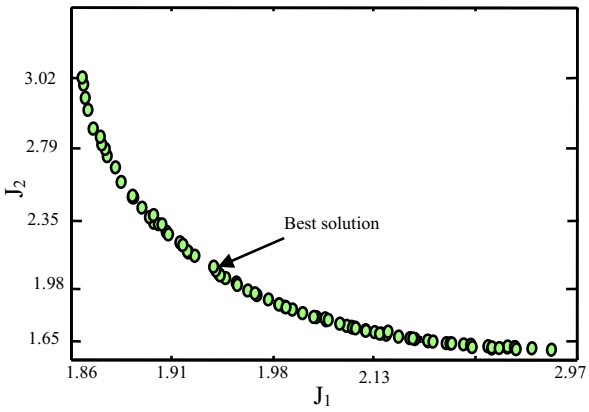

Fig. 11. Pareto-optimal fronts of the proposed algorithm

According to Fig. 10, the input signals of the fuzzy controller are in the range [-2, +2]. These signals are errors and the changes of errors. Due to the operating conditions as given in Table 1, some parameters is increased and decreased. At first, we evaluate these parameters effects on the plant's output to select worst operating conditions in designing the proposed fuzzy P-PID controller. The effects of these parameters on the frequency fluctuations are shown in Fig. 12.

It can be observed that two parameters R and TDEG have a similar performance when the overshoot is enhanced up to +40%; they are increased. On the other hand, two parameters TWTG and (d) TPV have same effects when they are decreased to -40%. In addition, to demonstrate the robustness of the proposed control strategy, two performance indices ITAE and FD are defined as follows:

$$ITAE = 100 \int_0^{t_{sim}} t.(|\Delta f|)dt \tag{23}$$

$$FD = \alpha_{os} \times OS + \alpha_{us} \times US + \alpha_{t_s} \times T_s \tag{24}$$

where, OverShoot (OS), UnderShoot (US) and settling time of the MG frequency deviation are considered for the FD evaluation.

It is worth noting that the lower values of these indices shows the better response of MG system control in terms of time-domain characteristics. Parameters aos, aus and ats are penalty factors to make equal values for OS, US and Ts, respectively. To the reader easily the fuzzy surface and fuzzy inference diagrams are shown in Figs. 13 and 14, respectively. Synchronizing these factors make better comparison based on FD value.

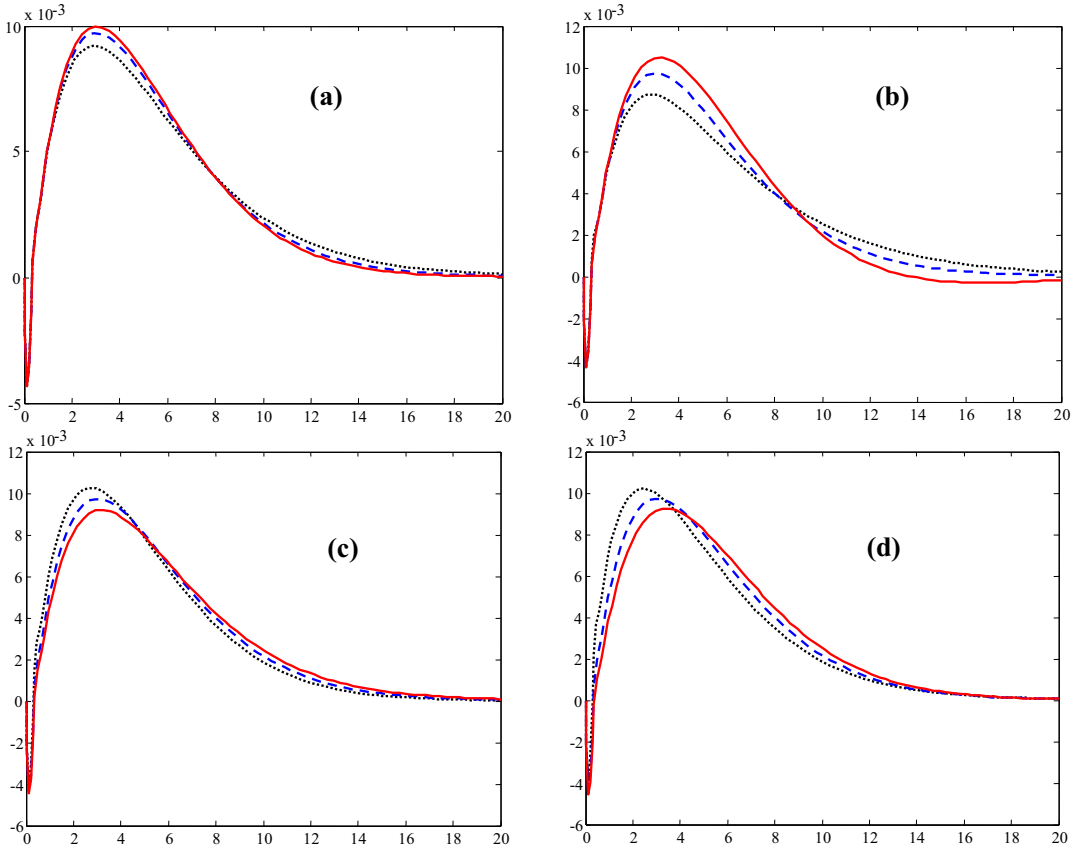

Fig. 12. Effects of different parameters on frequency stability between -40% to +40 %, (a) R (b) TDEG (c) TWTG and (d) TPV, +40% (Solid), 0% (Dashed) and -40% (Dotted)

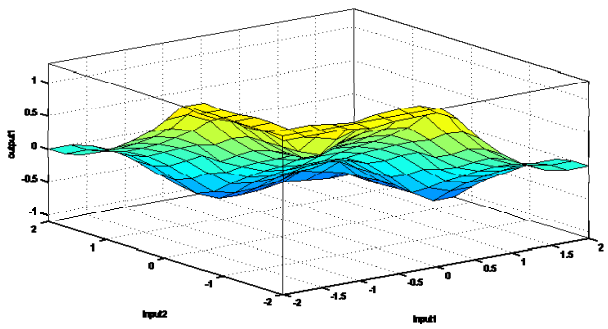

Fig. 13. Graphical view of fuzzy surface

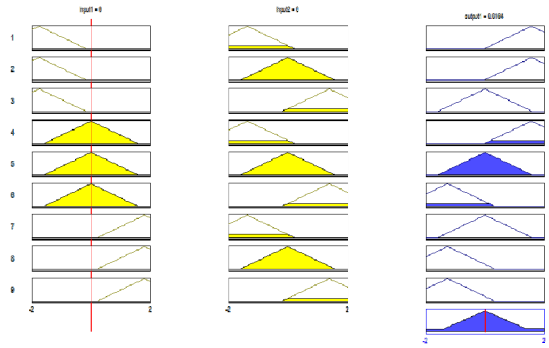

Fig. 14. Fuzzy inference diagram

To shows the robustness and effectiveness of the proposed controller, it compared with the following controllers in different operating conditions:

1. Conventional PID controller
2. Multi-stage fuzzy controller [30]

As the first evaluation, the load step ΔPL = 0.1 as an external fault is added to the studied MG as shown in Fig. 2. The responded frequency oscillation is shown in Fig. 15. It can be seen that the overshoot in the equipped system with fuzzy P-PID controller is significantly better than two other methods. Moreover, undershoot in the proposed controller is completely removed and the settling

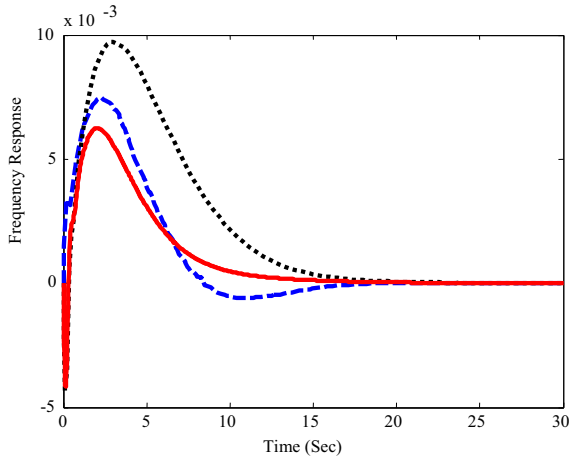

Fig. 15. Frequency response of the microgrid with the load step 0.1 without delay, Fuzzy P-PID (Solid), Multi stage (Dashed) and PID (Dotted)

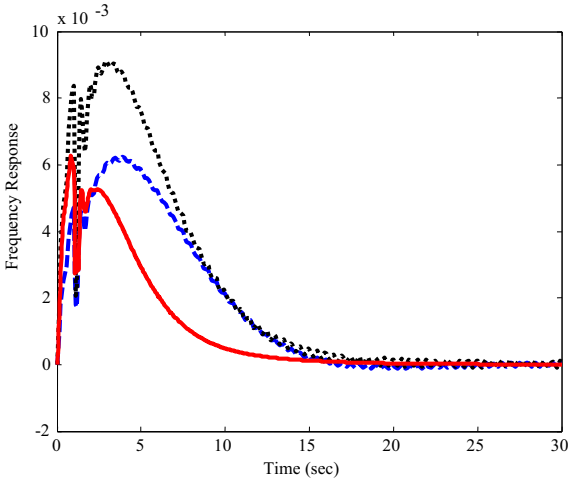

Fig. 16. Frequency response of microgrid with the load step 0.1 with delay, Fuzzy P-PID (Solid), Multi-stage (dashed) and PID (Dotted)

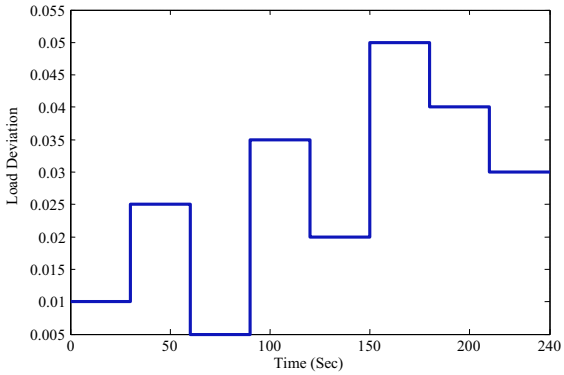

Fig. 17. The load step changes of the interval 240 s.

time is decreased from 16 s (best solution for two other controllers) to 11 s for the fuzzy P-PID controller.

To show the robustness of the proposed controller under different sever operating conditions; Fig. 16 presents the frequency response in MG under the load step 0.1 and delay block. It can be seen that the performance of the proposed controller is better than other methods.

It can be concluded from Figs. 14 and 16 that the proposed controller in each condition has a robust performance because the compared values of indices OS, US and Ts are close together. In order to show the accepted performance of the proposed algorithm, its results of are compared with PI and multi-stage fuzzy controllers under multi-step loadings as shown in Fig. 17 and its frequency response is shown in Fig. 18.

Figure 20 shows the frequency response of the MG under sever loading conditions consisting of random load power changes as shown in Fig. 19 with increasing the parameters R and TDEG to +40% of the nominal values and de-

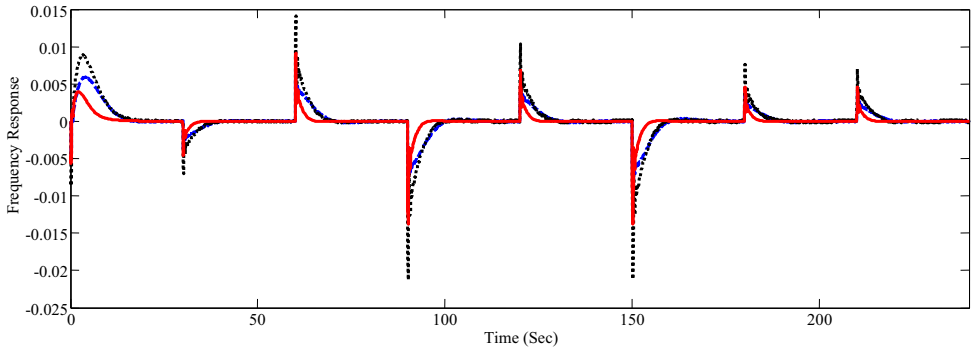

Fig. 18 . Frequency response of the microgrid to load step changes in the interval 240 s, Fuzzy P-PID (Solid), Multi stage (dashed) and PID (Dotted)

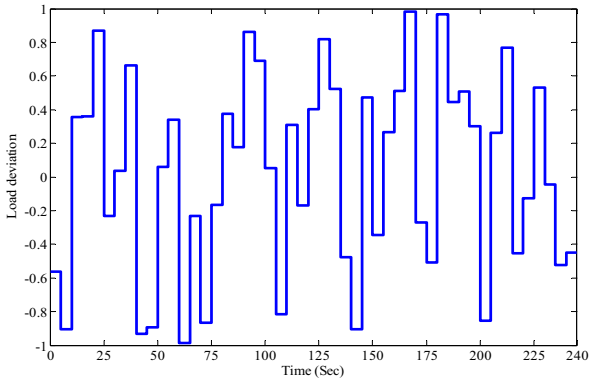

Fig. 19. Random load power change

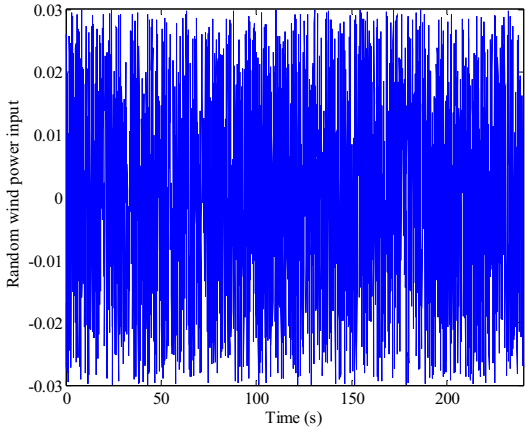

Fig. 21. Random wind power input

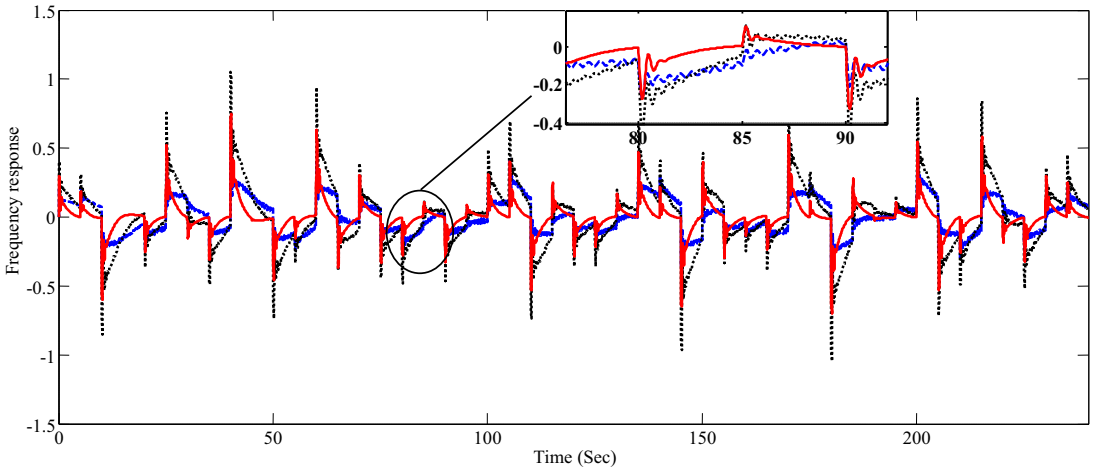

Fig. 20. System frequency deviation below 40% TWTG and TPV decreasing, 40% R and TDEG increasing and random load power change, Fuzzy P-PID (Solid), Multi-stage (dashed) and PID (Dotted)

creasing parameter TWTG and TPV to -40% of the nominal values. This case can be considered as the worst operating condition observed in the literature. In fact, successful performance under these conditions grantees the good performance of the proposed fuzzy P-PID controller in the real-time system.

To demonstrate the MG stability by random wind power input, assume that the wind input is varied as shown in Fig. 21. The system frequency response is shown in Fig. 22.

It can be seen from these figures that the frequency deviations of the MG are greatly reduced by the proposed fuzzy P-PID controller in terms of overshoot, undershoot and settling time. In other words, the proposed control strategy has a good and rather quick performance in

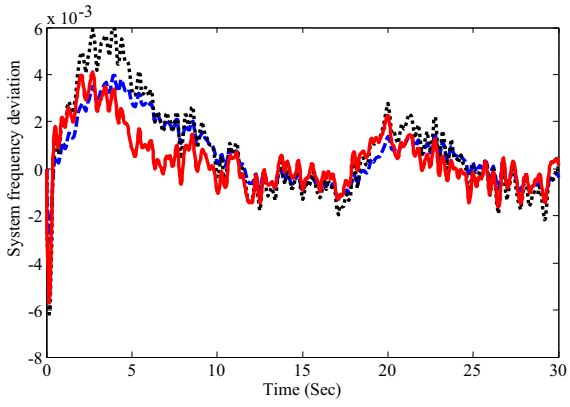

Fig. 22. System frequency deviation for random wind power input, Fuzzy P-PID (Solid), Multi stage (dashed) and PID (Dotted)

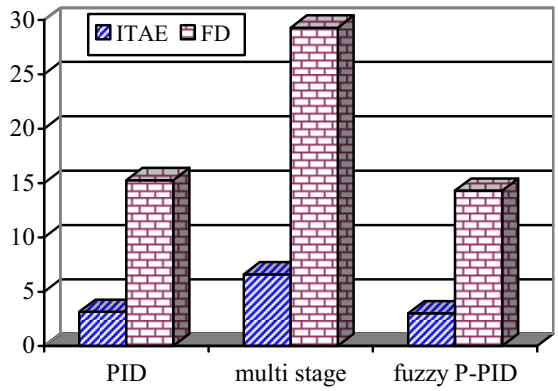

Fig. 23. Comparison values for microgrid without delay block

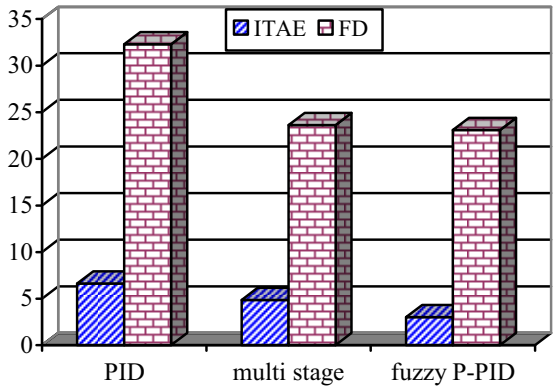

Fig. 24. Comparison values for microgrid with delay block

damping the frequency oscillations. Moreover, the numerical results for different cases are shown in Figs. 23 and 24. It is worth mentioning that the lower values of these indices shows better system response in terms of time domain characteristics. Therefore, it is clear that the performance of the MG equipped with the fuzzy P-PID controller is better than the conventional PID and multi stage fuzzy controllers.

In order to evaluate the robustness of the proposed controller, it is assumed that the solar irradiation is changed as shown in Fig. 25. Moreover, like sever operating conditions, the wind speed and load disturbance are also regarded as shown in Fig 25. In this case, the time-domain simulation result is depicted in Fig. 26. The value of Δf gradually returns to zero due to linear increases of Φ and PPV. It can be concluded that longer time constant in the studied system can filter out large fluctuations caused by the inherent random solar-irradiation variations. However, longer time delay has a detrimental effect on the controlling performance on the studied system.

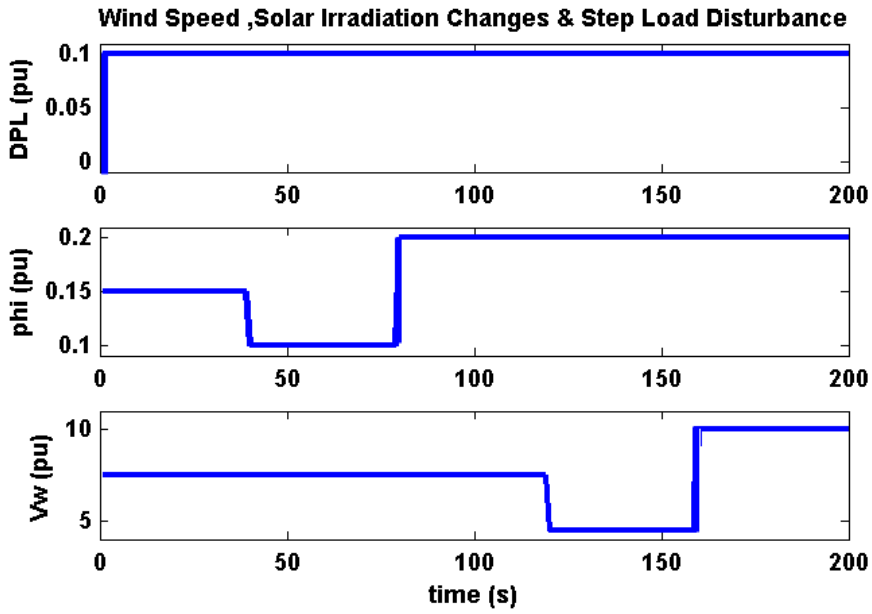

Fig. 25. Variation of solar irradiation, wind speed and load step disturbance

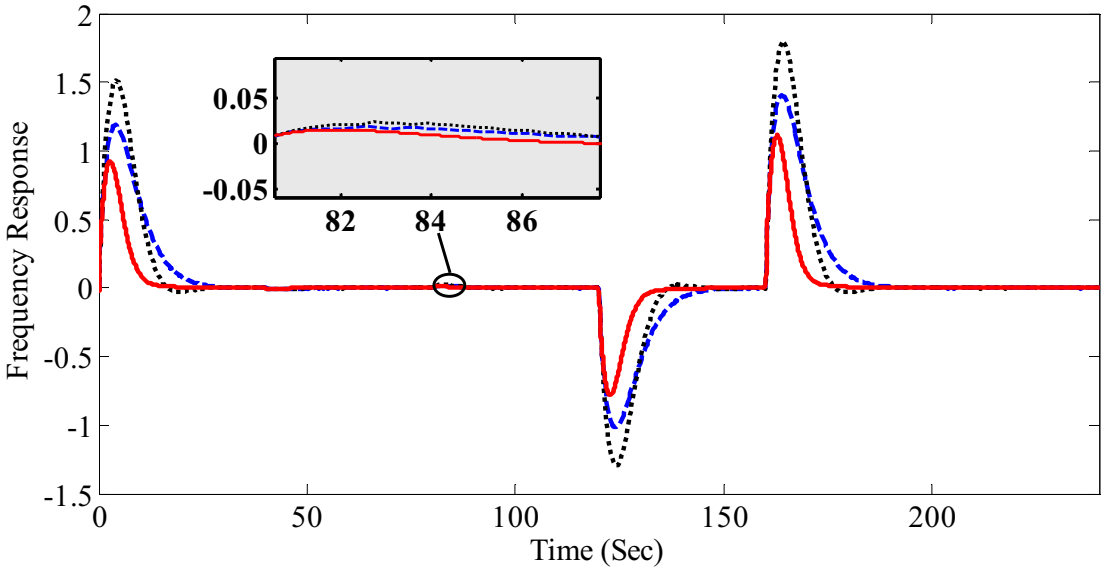

Fig. 26. System frequency deviations for random solar irradiation, wind speed, step load and +40 uncertainties, Fuzzy P-PID (Solid), Multi-stage (Dashed) and PID (Dotted)

6. Conclusions

This paper presents a robust design of the proposed and adaptive fuzzy P-PID controller for a microgrid system with different types of uncertainties (to convert this model to a practical microgrid) and power units (PV, wind, diesel and etc) in order to enhance the frequency deviation damping caused by MG performance under unexpected conditions. Unlike the conventional controller such as PID, the optimal tuning of fuzzy membership functions and rules is very essential for improving control system performance since a non-optimal set of membership functions and rules may lead to sever instability in a microgrid system. Hence, a multi-objective CGSA algorithm has been used to optimally tune the fuzzy set variables in the proposed fuzzy controller. Based on two conflicted objective functions in time and frequency domains, the proposed design problem is converted to a multi objective optimization problem over a wide range of loading conditions. According to the results obtained from the proposed algorithm, it can be said that it is an appropriate approach to improve the frequency deviation. Moreover, extensive simulation studies show that the proposed controller provides the desired closed loop performance over a wide range of operating conditions. The findings of this study contribute the researchers to find out the optimal tuning for frequency controller on microgrids. It is also a contribution to the existing knowledge on microgrids according to four following reasons:

1. An improved fuzzy P-PID controller is investigated for damping the frequency oscillations of microgrid.
2. The efficiency of the CGSA algorithm in comparison with other methods is proved.
3. The CGSA algorithm improved the fuzzy P-PID controller design efforts for frequency oscillations in microgrids.
4. Evaluations of the proposed controller effectiveness under different types of operating conditions such as changes in solar irradiation, wind speed, load step and microgrid uncertainties are indicative of its appropriate performance.

Appendix A: The microgrid data

All microgrid data are shown in Table 3.

Table 3. Microgrid system Data

Parameters	Value	Parameters	Value
R(Hz/pu)	3.0	K_{ae}	1.5
D(Hz/pu)	0.012	T_{ae} (s)	0.5
2H(pu s)	0.1667	K_{fc}	1.1
K_{deg}	1.3	T_{fc} (s)	4.0
T_{deg} (s)	2.0	K_{pv}	1.8
T_t (s)	0.3	T_{pv} (s)	1.0
T_{gi} (s)	0.3	K_{fess}	-1.1
K_{wtg}	1.0	T_{fess} (s)	0.1
T_{wtg} (s)	1.5	K_{bess}	-1.3
K_a	0.6	T_{bess} (s)	0.1

Appendix B: Algorithm convergence analysis

In this section, the exploitation and exploration of the proposed CGSA algorithm and how it performs better than the classical GSA by testing Langermann's function [31] with two variables of X1 and X2 known as a non-convex problem are presented. Note that this function has many local solutions different from global solutions identified by the smooth plate. To the convenience of the readers, a 3-D view of this function is shown in Fig. 27 and the mathematical equation is presented below:
Figure 28 shows the contour plot of Eq. (25) dealing with the movement of the population in the search process. It can be seen that all population in the proposed algorithm are focused on the global solution in last iteration but the GSA has some violations. According to this analysis, the standard deviations of CGSA and GSA are about 0.002 and 0.035, respectively

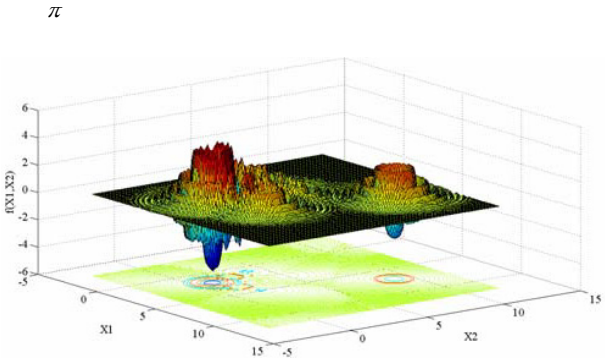

Fig. 27. 3-D graph of Langermann's function

$$f(x_1,x_2)=-\sum_{i=1}^{5}\frac{c_i\cos(\pi[(x_1-a_i)^2+(x_2-b_i)^2])}{\exp(\frac{(x_1-a_i)^2+(x_2-b_i)^2}{\pi})},\begin{cases}a=[3\quad 5\quad 2\quad 1\quad 7]^T, c=[1\quad 2\quad 5\quad 2\quad 3]^T\\ b=[5\quad 2\quad 1\quad 4\quad 9]^T\end{cases} \tag{25}$$

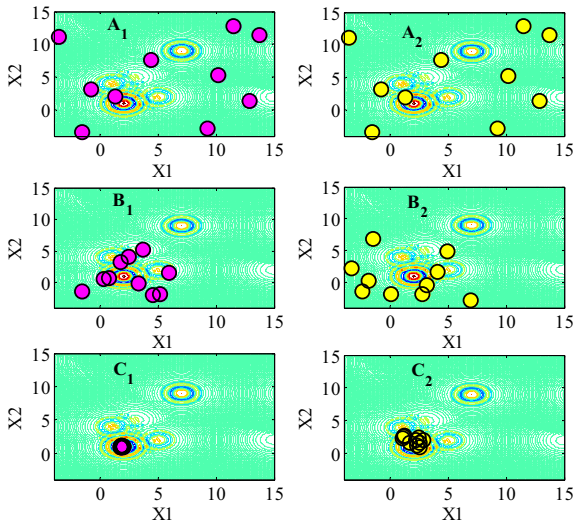

Fig. 28. A1-A2: Initial population in first iteration for CGSA and standard GSA, respectively, B1-B2: Movement of the population after 300th iteration, for CGSA and standard GSA, respectively, C1-C2: Movement of population after 300th iteration, for CGSA and standard GSA, respectively

Reference

[1] M. R. Khalghani, M. H. Khooban, E. Mahboubi-Moghaddam, N. Vafamand, and M. Goodarzi, *"A self-tuning load frequency control strategy for microgrids: Human Brain Emotional Learning"*, Electrical Power and Energy Systems, Vol. 75, pp. 311-319, 2016.

[2] M. Goyal, and A. Ghosh, *"Microgrids interconnection to support mutually during any contingency"*, Sustainable Energy, Grids and Networks, Vol. 6, pp. 100-108, 2016.

[3] A. Esmaeli, "*Stability analysis and control of microgrids by sliding mode control*", Electrical Power & Energy Systems", Vol. 78, pp. 22-28, 2016.

[4] C. Supriyadi, and A. Nandar, " *Robust PI control of smart controllable load for frequency stabilization of microgrid power system*", Renewable Energy, Vol. 56, pp. 16-23, 2013.

[5] T. S. Bhatti, A. A. F. Al-Ademi, and N. K. Bansal, "*Load frequency control of isolated wind diesel hybrid power systems*", Energy Conversion and Management, Vol. 39, pp. 829-837, 1997.

[6] M. H. Moradi, M. Eskandari, and S. M. Hosseinian, "*Cooperative control strategy of energy storage systems and micro sources for stabilizing microgrids in different operation modes*", Electrical Power & Energy Systems, Vol. 78, pp. 390-400, 2016.

[7] G. Shabib, "*Implementation of a discrete fuzzy PID excitation controller for power system damping*", Ain Shams Engineering Journal, Vol. 3, pp. 123-131, 2012.

[8] A. Menadi, S. Abdeddaim, A. Ghamri, and A. Betka, "*Implementation of fuzzy-sliding mode based control of a grid connected photovoltaic sys-*

tem", ISA Transactions, Vol. 58, pp. 586-594, 2015.

[9] I. A. Dounis, P. Kofinas, C. Alafodimos, and D. Tseles, "*Adaptive fuzzy gain scheduling PID controller for maximum power point tracking of photovoltaic system*", Renewable Energy, Vol. 60, pp. 202-214, 2013.

[10] H. Shayeghi, A. Ghasemi, and H. Shayanfar, "*PID type stabilizer design for multi machine power system using IPSO procedure*", Computer Science and Engineering, Vol. 1, No. 2, pp. 36-42, 2011.

[11] A. Zakariazadeh, and Sh. Jadid, "*Integrated Scheduling of Electric Vehicles and Demand Response Programs in a Smart microgrid*", Iranian Journal of Electrical and Electronic Engineering", Vol.10, No. 2, pp.114-123, 2014.

[12] A. Hajizadeh, "*Robust Power Control of microgrid based on Hybrid Renewable Power Generation Systems*", Iranian Journal of Electrical and Electronic Engineering, Vol. 9, No. 1, pp. 44-57, 2013.

[13] J. Li and P. Li, "*Research on microgrid frequency control with droop characteristic based on lagrange interpolation*", Applied Mechanics and Materials, Vol. 556-562, pp. 1814-1817, 2014.

[14] F. D. Mohammadi, M. J. Ghorbani, A. Feliachi and M. A. Choudhry, "*Novel load frequency control approach based on virtual area error in a microgrid including PV and battery*", IEEE PES General Meeting, Conference & Exposition , National Harbor, 2014.

[15] M. F. M. Arani and Y. A. I. Mohamed, "*Analysis and impacts of implementing droop control in DFIG-based wind turbines on microgrid/weak-grid stability*", IEEE Transactions on Power Systems, Vol. 30, No. 1, pp. 385-396, 2015.

[16] C. Yuen, A. Oudalov and A. Timbus, "*The provision of frequency control reserves from multiple microgrids*", IEEE Transactions on Industrial Electronics, Vol. 58, No. 1, pp. 173-183, 2011.

[17] N. Rezaei and M. Kalantar, "*Economic-environmental hierarchical frequency management of a droop-controlled islanded microgrid*", Energy Conversion and Management, Vol. 88, p. 498–515, 2014.

[18] M. F. Kangarlu and M. A. Pahlavani, "*Cascaded multilevel converter based superconducting magnetic energy storage system for frequency control*", Energy, Vol. 70, pp. 504-513, 2014.

[19] K. Singh, C. Singh and N. K. Yadav, "*Load frequency control in microgrid*", International Journal in Computer and Communication Technology, Vol. 2, No. 9, pp. 680-684, 2013.

[20] S. Vachirasricirikul and I. Ngamroo, "*Robust LFC in a smart grid with wind power penetration by coordinated V2G control and frequency controller*", IEEE Transaction on Smart Grid, Vol. 5, No. 1, pp. 371-380, 2014.

[21] X. Li, Y. J. Song and S. B. Han, "*Frequency control in micro-grid power system combined with electrolyzer system and fuzzy PI controller*", Journal of Power Sources, Vol. 180, No. 1, pp. 468-475, 2008.

[22] C. Lung, T. Shinta, H. Kakigano and Y. Miura, "*Control of uninterrupted switching using a virtual synchronous generator between stand-alone and grid-connected operation of a distributed generation system for houses*", Electrical Engineering in Japan, Vol. 190, No. 4, pp. 26-36, 2015.

[23] I. Serban and C. Marinescu, "*Battery energy storage system for frequency support in microgrids and with enhanced control features for uninterruptible supply of local loads*", Electrical Power and Energy Systems, Vol. 54, pp. 432-441, 2014.

[24] Q. Shafiee, J. M. Guerrero and J. C. Vasquez, "*Distributed secondary control for islanded microgrids - z novel approach*", IEEE Transactions on Power Electronic, Vol. 29, No. 2, pp. 1018-1031, 2014.

[25] A. Ghasemi, H. Shayeghi, and H. Alkhatib, "*Robust design of multimachine power system stabilizers using fuzzy gravitational search algorithm*", Electric Power Energy Systems, Vol. 51, pp. 190-200, 2013.

[26] H. Shayeghi, and A. Ghasemi, "*A modified artificial bee colony based on chaos theory for solving non-convex emission/economic dispatch*", Energy Conversion and Management, Vol. 79, pp. 344-35, 2014.

[27] H. Shayeghi, and A. Ghasemi, "*Optimal tuning of PID type stabilizer and AVR gain using GSA technique*", International Journal on Technical and Physical Problems of Engineering , Vol. 4, No. 2, pp. 98-106, 2012.

[28] H. Bevrani, F. Habibi, P. Babahajyan, M. Watanabe, and Y. Mitani, "*Intelligent frequency control in an AC microgrid: online PSO-based fuzzy tuning approach*", IEEE Transactions on Smart Grid, Vol. 3, pp. 1935-1944, 2012.

[29] A. Ghasemi, "*A fuzzified multi objective interactive honey bee mating optimization for environmental/economic power dispatch with valve point effect*", Electrical Power and Energy Systems, Vol. 49, pp. 308-321, 2013.

[30] O. Abedinia, N. Amjady, A. Ghasemi, H. Shayeghi, "*Multi-Stage fuzzy load frequency control based on multiobjective harmony search algorithm in deregulated environment*", Journal of Operation and Automation in Power Engineering, Vol. 1, No. 1, pp. 63-73, 2013.

[31] http://infinity77.net/global_optimization/test_functions_nd_L.html

Hossein Shayeghi received the B. S. and M. S. E. degrees in Electrical and Control Engineering in 1996 and 1998, respectively. He received his Ph.D. degree in Electrical Engineering from Iran University of Science and Technology, Tehran, Iran in 2006. Currently, he is a full Professor in Technical Engineering Department of University of Mohaghegh Ardabili, Ardabil, Iran. His research interests are in the application of robust control, artificial intelligence and heuristic optimization methods to power system control design, operation and planning, power system restructuring and smart grids. He has authored and co-authored of 6 books in Electrical Engineering area all in Farsi, one book and four book chapters in international publishers and more than 345 papers in international journals and conference proceedings. Also, he collaborates with several international journals as reviewer boards and works as editorial committee of eight international journals. He has served on several other committees and panels in governmental, industrial, and technical conferences. He was selected as distinguished researcher of the University of Mohaghegh Ardabili several times. In 2007 and 2010 he was also elected as distinguished researcher in engineering field in Ardabil province of Iran. Furthermore, he has been included in the Thomson Reuters' list of the top one percent of most-cited technical Engineering Scientists in 2015 and 2016, respectively. Also, he is a member of Iranian Association of Electrical and Electronic Engineers (IAEEE) and Senior member of IEEE.

Ali Ghasemi received the B.Sc. and M.Sc. (Honors with first class) degree from IUT, UMA, in 2009 and 2011, respectively. and, currently he is pursuing the Ph.D. degree in the electrical engineering and computer science of UMA. His research interests are application of forecast methods, operation adaptive and robust control of power systems, Planning, Power System Restructuring and applications of heuristic techniques. He has authored of a book in Electrical Engineering area, and more than 90 papers in reputable international journals and conference proceedings. Also, he collaborates as editorial committee and reviewer of 11 international journals. He is a member of the IAEEE. He has received some awards, including the Excellence in M.Sc thesis Award from EPGC and UMA, 2012 and 2013, the honors M.Sc. and Ph.D student of UMA, 2014, the best researcher from young researcher and Elite club, 2013.